Chemical Engineering Journal 151 (2009) 333–341

Contents lists available at ScienceDirect

Chemical Engineering Journal

journal homepage: www.elsevier.com/locate/cej

Characterization of chemical kinetics in membrane-based liquid–liquid extraction of molybdenum(VI) from aqueous solutions

H. Valdés[a], J. Romero[a,*], J. Sanchez[b], S. Bocquet[b], G.M. Rios[b], F. Valenzuela[c]

[a] *Laboratorio de Procesos de Separación por Membranas, Departamento de Ingeniería Química, Universidad de Santiago de Chile (USACH), Av. Lib. Bdo. O'Higgins 3363, Estación Central, Santiago, Chile*
[b] *Institut Européen de Membranes, UMR 5635, ENSCM, CNRS, UMII, Université de Montpellier II, France*
[c] *Departamento de Ciencia de los Alimentos y Tecnología Química, Facultad de Ciencias Químicas y Farmacéuticas, Universidad de Chile, Chile*

ARTICLE INFO

Article history:
Received 29 October 2008
Received in revised form 3 April 2009
Accepted 3 April 2009

Keywords:
Membrane contactor
Modelling
Liquid–liquid extraction
Molybdenum
Mass transfer

ABSTRACT

This study aims to describe the mass transfer in a membrane-based solvent extraction system for the extraction of molybdenum(VI) from aqueous solutions, identifying chemical kinetics of the complex formation at the interface. The analyzed process is the membrane-based solvent extraction of molybdenum(VI) from aqueous solutions with n-hexane containing Alamine 336 as extraction phase using a hollow fiber contactor. This extraction process has been described through a resistances-in-series model, taking into account transport and thermodynamic relationships. In this work, the model has been used to identify an effective reaction rate expression and to describe the mass transfer by complex formation at the interface. The reaction rate expression has been estimated from experimental data obtained in a previous work [F. Valenzuela, H. Aravena, C. Basualto, J. Sapag, C. Tapia, Separation of Cu^{2+} and molybdenum(VI) from mine waters using two microporous extraction systems, Separation Science and Technology 35 (2000) 1409–1421]. The proposed calculation methodology can be used as a tool to scale-up when the information about chemical kinetics of complex formation is not available.

1. Introduction

Pollution in soils and water generated by the presence of heavy metals represents an important problem, especially in regions where mining industry on a large scale is present. Generally, some elements as selenium, molybdenum or arsenic are not considered like heavy metals but in terms of pollution they can generally be qualified in this category. Up to now in the literature, separation or recovery processes of these elements (or compounds) have not been completely characterized.

Accumulation of heavy metals in downstream waters generates putrefaction of the flora and consumption of oxygen, which alters ecosystems and involves serious consequences to the human health [2].

Molybdenum is generally used in alloys because it contributes to increase the steel resistance at high temperatures and corrosion conditions. Molybdenum compounds are also used as catalysts in oil industry and processes involving dyes, plastics and rubber compounds as well as in different pigments (orange color) [3–5]. In the last years, the commercial value of this metal has been significantly increased due to the demand on the part of the emergent economies.

Currently, the extraction of heavy metals like molybdenum, from aqueous solutions is accomplished by solvent extraction (SX), but this process presents some disadvantages (e.g. large volumes of solvents, high operation costs, possible formation of emulsions, large equipments and high residence time).

Several authors report the solvent extraction of molybdenum using different solvents, extractants agents and types of contactor [6–15]. A vast body of literature has been published to describe membrane-based solvent extraction processes applied to the separation or purification of different types of compounds as metals, phenol compounds, organic acids, aroma compounds and pharmaceutical products [16–39]. An interesting alternative for extraction of molybdenum can be developed by means of membrane contactors. Among the most studied membrane-based extraction processes of molybdenum, liquid–liquid membrane contactors, supported liquid membranes (SLM) and emulsified liquid membranes (ELM) have been analyzed in different works [40–44].

In general, systems based on membrane contactors consider the use of hollow fibers modules [45–48]. This type of contactors offers great extraction efficiency and other several advantages, as such as, the available surface area remains undisturbed at high and low flow rates because the two fluid flows are independent, unlike traditional contactors, no density difference is required between

---

[*] Corresponding author. Tel.: +56 2 718 18 21; fax: +56 2 681 71 35.
E-mail address: julio.romero@usach.cl (J. Romero).

1385-8947/$ – see front matter © 2009 Elsevier B.V. All rights reserved.
doi:10.1016/j.cej.2009.04.012

Nomenclature

A	surface area (m^2)
a	kinetic parameter in Eq. (5)
b	kinetic parameter in Eq. (5)
C	concentration (mol L^{-1})
d	diameter (m)
D	diffusion coefficient (m^2 s^{-1})
e	thickness of fiber (m)
FR	fractional resistance
HTU	high transfer unit (m)
J	flux (mol s^{-1})
k	individual mass transfer coefficient (m s^{-1})
K_T	Boltzmann's constant (kg m^2 s^{-2} K^{-1})
k_1	chemical kinetics constant (mol$^{1-(a+b)}$ (cm^3)$^{(a+b)}$ s^{-1})
L	length (m)
M	mass molar (kg mol^{-1})
Mo	Mo(VI) as molybdenite
MoR	complex
p	permeate side
P	permeability (m s^{-1})
Q	circulation rate (L s^{-1})
Re	Reynolds number
r	radius (m)
R	constant of gases (kg m^2 mol^{-1} K^{-1} s^{-2})
Sh	Sherwood number
Sc	Schmidt number
T	temperature (K)
x	molar fraction

Greek letters

ρ	density (kg m^{-3})
μ	viscosity (kg m^{-1} s^{-1})
ν	velocity (m s^{-1})
Δ	gradient
ε	porosity
τ	tortuosity
λ	free mean path (m)

Subscripts

aq	aqueous solution
aqueous	referred to aqueous solution
A	component A
B	component B
ET	outside diameter of fibers
eq	hydraulic diameter
fiber	referred to fibers
i	component i
IT	inside diameter of the fiber
kinetic	referred to complex formation at the interface
membrane	referred to membrane pores filled with organic phase
Mo	metal ion
$\mathrm{Mo_i}$	metal ion (at the interface)
m	membrane
org	organic phase
organic	referred to organic solution
P	membrane pore
$\mathrm{R_3N_i}$	Alamine 336 (at the interface)
$\mathrm{R_3N_p}$	Alamine 336 (at the pore entrance)
S	shellside
shell	referred to shell
T	tube or lumenside

fluids, interfacial area is known and is constant, which allows performance to be predicted more easily than with conventional dispersed phase contactors. The scale-up of membrane contactors can be practically linear.

The analysis of extraction processes using membrane contactors requires the integration of mass transfer equations and chemical kinetics relationships, which must describe the complexation rate at the interface. This approach can represent a disadvantage in order to describe the operation because the reaction rates are not always well known [49,50].

The main goal of this study is to describe the overall mass transfer of molybdenum(VI) in a membrane extraction process using hollow fibers contactors and the application of these results to identify a general relationship of the complexation rate at the interface explaining the formation rate of the metal–extractant complex. This approach is proposed as a generalized description of membrane-based solvent extraction of metals, which may be applied to identify chemical kinetics and phenomenological aspects in a first step, and to design and scale-up this type of systems in a future step.

2. System studied

In this study is developed a resistances-in-series model for the simulation of an extraction system of molybdenum(VI) from liquid effluents by means of a liquid–liquid membrane contactor, when the rate of the complex formation is not known. The model considers the correlation of a local kinetics relationship from experimental data and its integration in a resistances-in-series model.

The macroporous membrane used in this process is hydrophobic and in consequence the aqueous solution cannot penetrate in the pores, which is filled with the extraction solvent. Therefore, aqueous–organic interface is stabilized at the entrance of the pores and molybdenum(VI) present in the aqueous phase as molybdenite will be extracted by complexation at this interface. Fig. 1 shows an outline of mass transfer for this process, where molybdenite is transported from the aqueous solution to the organic one by means of four steps: (1) transport through the aqueous boundary layer; (2) complexation and transfer with the extractant agent at the interface; (3) diffusion of complex within the pores filled with organic phase; (4) transport through the organic boundary layer. The concentration profiles of molybdenite [Mo(VI)], extractant [$\mathrm{R_3N}$], and complex [MoR], are schematically presented in Fig. 1.

2.1. Description of the membrane contactor process

The system studied in this work is a membrane-based solvent extraction using a hollow fiber contactor (HFC). The goal of this extraction operation is the removal of molybdenum(VI) from an aqueous solution using an organic extraction solution of Alamine 336 in n-hexane. Experimental data used in this work to validate the proposed model developed herein was obtained and presented by Valenzuela et al. in a previous work [1].

In those experiments, an acid aqueous solution of Mo(VI) as molybdenite was circulated in the lumenside of a hollow fiber contactor. Membrane extractor was built using a reactor comprised of a glass shell and three hollow fibers made of polytetrafluoroethylene (PTFE). Hollow fibers were supplied by Japan Goretex Co. Organic extraction solution was circulated co-currently outside the fibers in order to maximize the stability of the interface decreasing the trans-membrane pressure drop that could be generated if counter-current mode were applied. Masterflex microtube pumps were used to circulate the aqueous feed and the organic extraction solution through the contactor. Operation pressure was controlled to maintain the stability of the interface at the pore entrance ($P_{\mathrm{fiber}} = P_{\mathrm{shell}} + 3$ psi). Operation variables and structural parameters of the extractor system are summarized in Table 1.

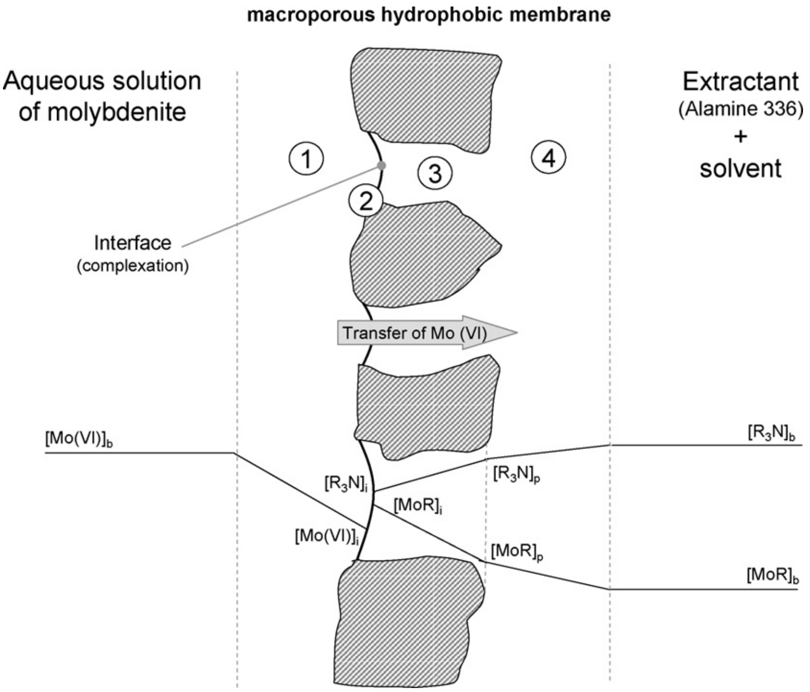

Fig. 1. Outline of mass transfer and concentration profiles of molybdenite (Mo(VI)), extractant (R_3N) and complex (MoR) in the proximities of the membrane. Subscripts 'b', 'p' and 'i' are related to bulk conditions, pore entrance and the interface, respectively.

The organic solution was prepared by dissolving tri-(C_8–C_{10}) amine (Alamine 336) in n-hexane. An acid leach residual solution of MoS_2 concentrate with nitric acid, provided by El Salvador Division of Copper Corporation of Chile (CODELCO), was used as the feed molybdenum-donor solution. Residual solutions considered in those experiments contain 1.0 g/L of molybdenum, 0.4 g/L of copper, 0.4 g/L of iron, 0.1 g/L of rhenium and minor concentration of other non-valuable metals. The pH was continuously adjusted to a suitable value for metal recovery and especially to prevent iron precipitation when the nitric acid leach residual solution was employed.

The main goal of this work involves the identification of the effective kinetic of the complex formation at the interface; these results could be applied to different process under different circulation modes and hydrodynamic conditions. An outline of this operation is presented in Fig. 2.

The pores of hydrophobic PTFE fibers are impregnated with the organic phase and the aqueous–organic interface is stabilized at the pore entrance on the lumenside. In this way, the mass transfer of molybdenum(VI) can be described by four steps:

(1) transfer of molybdenite through the boundary layer of aqueous phase to be treated in the lumenside;
(2) reaction of complex formation at the aqueous–organic interface, where the complexation of molybdenite can be described by the following global reaction:

$$(R_3N)_{org} + (H_2MoO_4)_{aq} \Leftrightarrow (R_3NH^+)(HMoO_4^-)_{org} \qquad (1)$$

(3) diffusion of the complex in the membrane pores filled with organic phase;
(4) transfer of the complex through the boundary layer of organic extraction phase in the shellside.

Table 1
Structural parameters of the membrane contactor system.

Property	Value	Unit
Circulation rate of aqueous solution	1.5×10^{-2}	$mL\,s^{-1}$
Circulation rate of organic solution	1.5×10^{-2}	$mL\,s^{-1}$
Number of fibers	3	–
ID of the fiber	10^{-3}	m
OD of the fiber	1.8×10^{-3}	m
Length	0.12	m
Internal diameter of the shell	0.015	m
Length of the shell	0.12	m
Porosity	0.60	–
Tortuosity	1.67	–
Surface area for mass transfer inside the fiber	1.13×10^{-3}	m^2
Surface area for mass transfer outside the fiber	2.04×10^{-3}	m^2
Surface area of flow in the lumenside	2.36×10^{-6}	m^2
Surface area of flow in the shellside	1.69×10^{-4}	m^2
Hydrodynamic diameter	1.06×10^{-2}	m

2.2. Formulation of the mass transport model

Few assumptions and considerations have been taken into account to apply a resistances-in-series approach to describe the overall mass transfer through the membrane, which is controlled by the four steps detailed in Fig. 1. This model was based on the following assumptions:

(a) aqueous and organic phases are completely immiscible;

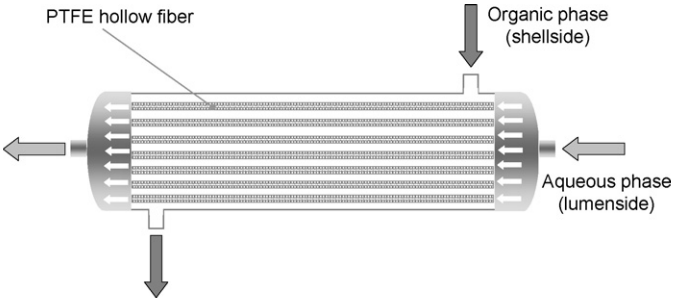

Fig. 2. Description of the hollow fiber membrane contactor used in experimental runs by Valenzuela et al. [1].

(b) the solutions are diluted and hydrodynamic properties are very close to the values of solvents (water and n-hexane). These physical properties have been considered constant;
(c) the system works under steady-state conditions. Nevertheless, experimental data used for parameter estimation have been obtained under transient conditions, but using large volumes of solutions with stable values of the concentrations in the time;
(d) reaction is limited at the aqueous–organic interface;
(e) circulation rates of the solutions in the membrane contactor are under laminar flow conditions.

In the next sections, mass transfer equations of each step described in Section 2.1 are developed.

2.2.1. *Mass transfer through the aqueous solution boundary layer*

According to assumptions b, e, and f, the flow of Mo(VI) (J_m, mol s^{-1}) through the boundary layer of the aqueous solution circulating on the lumenside can be estimated by Eq. (2):

$$J_m = k_{Mo} S_l (C_{Mo} - C_{Mo_i}) \tag{2}$$

where k_{Mo} is the mass transfer coefficient, S_l is the surface area available for mass transport on the lumenside; C_{Mo} and C_{Mo_i} are the concentrations of molybdenite at bulk and interface conditions, respectively.

The prediction of the mass transfer coefficient, k_{R3N}, in the lumenside has been done by means of the well-known equation of Sieder and Tate [51] for laminar regime, where the Sherwood number is given by the following correlation:

$$\mathrm{Sh_T} = 1.86\left(\mathrm{Re_T Sc_T}\frac{d_T}{L_T}\right)^{1/3} \tag{3}$$

2.2.2. *Complex formation at the interface*

In order to fit an effective relationship to estimate the reaction rate of the complex formation at the aqueous–organic interface described by Eq. (1), a simple kinetics equation can be proposed:

$$r = k[\mathrm{Mo}]_i^a [\mathrm{R_3N}]_i^b \tag{4}$$

In Eq. (5), r represents the reaction rate (mol s^{-1}); $[\mathrm{Mo}]_i$ and $[\mathrm{R_3N}]_i$ are the concentrations (mol L^{-1}) of Mo(VI) and Alamine 336 at the interface, respectively.

This rate of the complex formation at the interface may be modified by the pH value, but in the experimental runs [1] considered to validate the model developed in this study its value was continuously adjusted to pH 2.0.

2.2.3. *Diffusion through the membrane pores*

When the pores of a macroporous membrane are filled with stagnant liquid, the most probable mechanism to describe the mass transfer is molecular diffusion. The flow (mol s^{-1}) of Alamine 336 through the membrane pores can be estimated by the following equation:

$$J_m = \frac{D_{R_3N}\varepsilon}{l\tau} S_{ave}(C_{R_3N_p} - C_{R_3N_i}) \tag{5}$$

where ε is the porosity, l is the thickness and τ is the tortuosity. In this case, the mass transfer flow of extractant represents the mass transfer of complex, since under steady-state conditions, the amount of moles of complex transferred from the interface to the bulk of the organic phase would be considered identical to the amount of moles of extractant transferred from the bulk to the interface. This assumption is valid if the stoichiometry of the complex formation is described in Eq. (1).

Diffusion coefficient can be estimated by means of the Stoke–Einstein equation [52]:

$$D = \frac{k_B T}{6\pi r\mu} \tag{6}$$

where parameters k_B, r and μ are the Boltzmann constant, molecular radius and viscosity, respectively. From Eq. (6), the values of the diffusion coefficient of molybdenite in aqueous solution and Alamine 336 in organic phase are 9.31×10^{-6} and 5.08×10^{-6} cm^2 s^{-1}, respectively.

2.2.4. *Mass transfer through the organic solution boundary layer*

Mass transfer of the molybdenite-extractant complex through the boundary layer on the organic phase side can be described applying the same assumptions considered on the side of the aqueous solution to obtain Eq. (2).

Under steady-state conditions and taking into account the stoichiometry of the complex formation, the flow of Mo(VI) (as complex) through the boundary layer of the organic phase can be equalized to the counter-flow of extractant to the interface. Then, the effective flow of Mo(VI) through the boundary layer is given by

$$J_m = k_{R_3N} S_{shell}(C_{R_3N_b} - C_{R_3N_p}) \tag{7}$$

where k_{R3N} represents mass transfer coefficient of extractant on the organic boundary layer, S_{shell} is the mass transport surface area in the shellside; $C_{R_3N_b}$ and $C_{R_3N_p}$ are the concentrations of extractant in the bulk of the extraction solution and at the pore entrance, respectively.

Several correlations for mass transfer coefficient have been proposed in literature for hollow fiber contactors and presented in a review reported by Gabelman and Hwang [45]. These correlations were tested in this work, identifying two equations capable to estimate mass transfer liquid–liquid membrane contactors when a solution is circulated into a shell without baffles.

If $0.11 < \mathrm{Re} < 7.3$, the correlation proposed by Viegas et al. [53] can be applied to estimate the value of Sherwood number on the shell-side in function of Reynolds and Schmidt numbers, considering the values of hydrodynamic diameter (d_H) and the length of the membrane module (L). This relationship is represented by the following equation:

$$\mathrm{Sh_S} = 8.71\left(\frac{d_H}{L}\right) Re_S^{0.74} \mathrm{Sc}_S^{1/3} \tag{8}$$

This correlation was obtained by the Wilson-plot method, which has proved to be suitable for systems operating at steady-state conditions and where the only variable is the fluid velocity. Eq. (8) has been analyzed and applied to describe mass transfer rate on the shell-side in different systems with hollow fibers membrane contactors [23–27,53]. The good agreement of this equation with experimental information represents the main reason of choice.

Finally, Eqs. (2), (4), (5) and (7) must be equalized to calculate transmembrane flow at steady-state conditions.

2.3. *Physical properties of aqueous and organic solutions*

Values of density and viscosity of aqueous solutions of molybdenite at 30 °C have been reported by Valenzuela et al. [1] they are summarized in Table 2.

Properties of the organic extraction phase as density and concentration of extractant were directly obtained from data reported by Valenzuela et al. [1] as well as the viscosity of the Alamine 336.

On the other hand, the viscosity of organic solution was calculated by means of Eq. (9) proposed by Kendall and Monroe [54]:

$$\mu_m = [x_1\mu_1^{1/3} + x_2\mu_2{}^{1/3}]^3 \tag{9}$$

Table 2
Physical properties of the feed and extraction solutions.

Property	Aqueous phase	Organic phase	Unit
Density	1050	654	$kg\,m^{-3}$
Viscosity	9.00×10^{-4}	3.32×10^{-4}	$kg\,m^{-1}\,s^{-1}$
Temperature	303	303	K
pH	1.6	–	–
$[Mo]_b$	6.25×10^{-3}	–	$mol\,L^{-1}$
$[R_3N]_b$	–	0.042–0.167	$mol\,L^{-1}$

where μ_m represents the viscosity of the solution; μ_i and x_i are the viscosity and molar fraction of each compound (n-hexane and Alamine 336), respectively.

Values of the diffusion coefficient of molybdenite in water as well as the diffusion coefficient of Alamine 336 and complex (MoR) in n-hexane have been calculated by means of Stoke–Einstein equation [53]. Molecular radius of compounds required for estimation of diffusion coefficients are reported by Marchese et al. [41]. The molecular radius of molybdenite and Alamine 336 are 2.65×10^{-10} and 1.33×10^{-9} m, respectively.

3. Determination of chemical kinetics at the interface

Experimental data reported in a previous work by Valenzuela et al. [1] has been used in this work to fit a kinetics relationship for complex formation at the aqueous–organic interface. The experiments have been done in order to analyze the effect of the concentrations of extractant on the molybdenite transmembrane flow.

A correlation of interfacial concentrations, which were calculated from experimental data, was applied to obtain a chemical kinetics relationship describing the rate of complex formation at the interface according to Eq. (4). Interfacial concentrations and its correlation have been estimated by means of the following steps:

(1) Considering experimental values of flow of Mo(VI) reported in the literature [1] and taking into account the operation conditions of these experiments, concentration value of Mo(VI) at the interface (aqueous phase) is calculated by means of Eq. (2).
(2) Using the concentration of Mo(VI) at the interface estimated by Eq. (2), and the same values of experimental transmembrane flow, concentration of extractant agent (Alamine 336) at the pore entrance on the side of organic phase was estimated by means of Eq. (7).
(3) Under the same conditions, concentration of extractant at the interface (organic phase) was calculated by Eq. (5).
(4) With the concentration values of Mo(VI) and extractant agent estimated using Eqs. (2), (5) and (7), it is possible to correlate mass transfer flow of Mo(VI) through the interface using Eq. (4), obtaining a chemical kinetics relationship at the interface in function of parameters *k*, *a* and *b*. These parameters were calculated by multiple regressions using Labfit®.

Experimental values of transmembrane flow of Mo(VI) as molybdenite in function of concentration of extractant in the organic phase reported by Valenzuela et al. [1] are summarized in Table 3.

Kinetics relationship fitted in this work was obtained from averages experimental values of Mo(VI) flow because the system worked in transient regime with recirculation of solutions. However, this operation configuration involved a weak modification of the concentration – less than 2% related to the initial value – during the experiment extent.

Table 3
Experimental values of transmembrane flow of Mo(VI) obtained for different concentrations of Alamine 336 in extraction organic phase [1].

$[R_3N]$ ($mol\,L^{-1}$)	Flux of Mo(VI) ($mol\,m^{-2}\,s^{-1}$) $\times 10^5$
0.042	0.99 ± 0.05
0.061	1.08 ± 0.06
0.083	1.19 ± 0.06
0.099	1.27 ± 0.07
0.135	1.40 ± 0.05
0.167	1.61 ± 0.08

4. Simulation algorithm to prediction of the mass transfer

Once defined a kinetics relationship of the complex formation at the interface, a resistances-in-series model may be applied to estimate mass transfer of molydenite from the aqueous solution to the organic solution. This model represents the overall mass transport considering local resistances of each step described in Section 2.2 by means of Eqs. (2), (4), (5) and (7).

Resistances-in-series model is solved estimating the interfacial concentrations that involve the steady-state condition when Eqs. (2), (4), (5) and (7) represent the same value of the flow obtained by mass transfer and kinetics equation ($J_m = r$).

The algorithm applied to identify values of interfacial concentrations and flows is represented by the diagram presented in Fig. 3, which explains iterative calculations. The rate of convergence to the root representing the steady-state condition is accelerated applying a Regula Falsi method between an initial interval of interfacial concentrations.

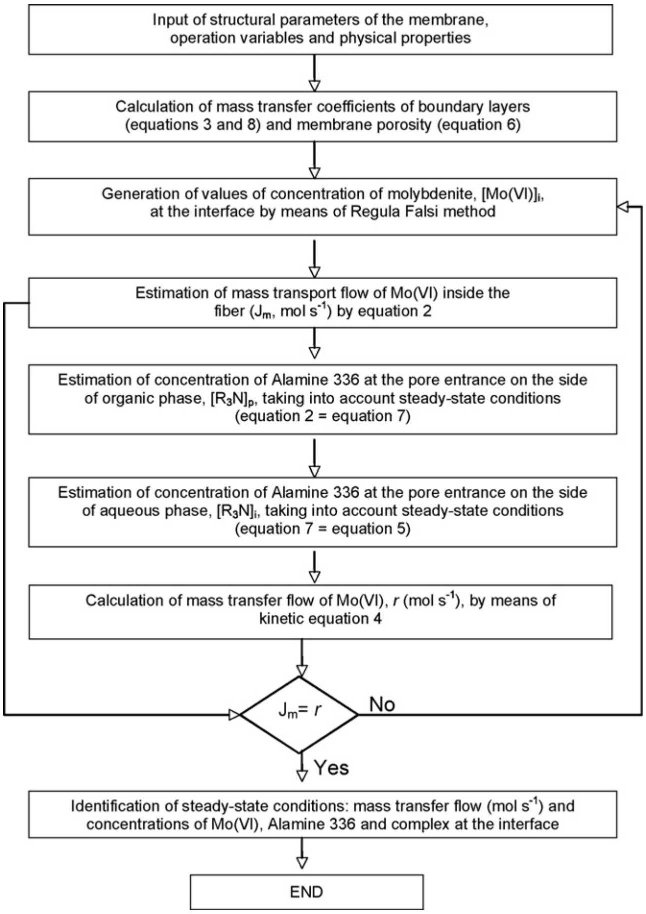

Fig. 3. Outline of the simulation algorithm applied in this work.

When the iterative cycle defined in the diagram presented in Fig. 3 identify the root or interfacial concentration that fulfills the steady-state condition ($J_m = r$). A program developed in Matlab® allows carrying out this calculation and to print the value of extraction percentages in a final step.

5. Determination of the rate-controlling steps

According to the resistances-in-series model proposed to describe the mass transfer through the membrane, the rate-controlling steps can be identified by means of the quantification of the fractional resistances of the respective step to the overall transport process. Juang and Chen [34] reported the estimation of fractional resistances in the extraction of citric acid using a supported liquid membrane. These calculations can be adapted to the system studied in this work. Thus, the flow of Mo(VI) under extreme conditions through the aqueous boundary layer, the aqueous–organic interface, the pores (organic), and the organic boundary layer is given by Eqs. (10)–(13), respectively.

$$(J_m)_{\text{aqueous}} = k_{\text{Mo}} S_l (C_{\text{Mo}}) \tag{10}$$

$$(J_m)_{\text{kinetic}} = r = k C_{\text{Mo}}^{a} C_{\text{R}_3\text{N}_b}^{b} \tag{11}$$

$$(J_m)_{\text{membrane}} = \frac{D_{\text{R}_3\text{N}}\varepsilon}{l\tau} S_{\text{ave}}(C_{\text{R}_3\text{N}_b}) \tag{12}$$

$$(J_m)_{\text{organic}} = k_{\text{R}_3\text{N}} S_{\text{Shell}}(C_{\text{R}_3\text{N}_b}) \tag{13}$$

The fractional resistances of the respective step to the overall mass transport process are calculated by means of Eqs. (14)–(17) from the values of J_m obtained by Eqs. (10)–(13):

$$R_{\text{aqueous}}(\%) = \frac{(1/J_m)_{\text{aqueous}}}{\{(1/J_m)_{\text{aqueous}} + (1/J_m)_{\text{kinetic}} + (1/J_m)_{\text{membrane}} + (1/J_m)_{\text{organic}}\}} \times 100 \tag{14}$$

$$R_{\text{kinetic}}(\%) = \frac{(1/J_m)_{\text{kinetic}}}{\{(1/J_m)_{\text{aqueous}} + (1/J_m)_{\text{kinetic}} + (1/J_m)_{\text{membrane}} + (1/J_m)_{\text{organic}}\}} \times 100 \tag{15}$$

$$R_{\text{membrane}}(\%) = \frac{(1/J_m)_{\text{membrane}}}{\{(1/J_m)_{\text{aqueous}} + (1/J_m)_{\text{kinetic}} + (1/J_m)_{\text{membrane}} + (1/J_m)_{\text{organic}}\}} \times 100 \tag{16}$$

$$R_{\text{organic}}(\%) = \frac{(1/J_m)_{\text{organic}}}{\{(1/J_m)_{\text{aqueous}} + (1/J_m)_{\text{kinetic}} + (1/J_m)_{\text{membrane}} + (1/J_m)_{\text{organic}}\}} \times 100$$

The rate-controlling steps of mass transfer can be quantitatively identified by comparing the above four values obtained from these equations.

6. Results and discussion

6.1. Prediction of the complexation rate at the interface

In this study is presented a simplified methodology to estimate effective chemical kinetic parameters in membrane-based solvent extraction of Mo(VI) applying well-known equations of mass transfer through boundary layers and membrane pores.

Kinetics relationships supposed for these calculations are arbitrary, but they allow fitting the rates of chelation at the interface. Nevertheless, any reaction mechanism of complex formation cannot be deduced from Eq. (4). Calculation of the parameters k, a and b in Eq. (4) was done by means of multiple regression of mass transfer flow in function of concentrations at the interfaces. The value obtained for the constant k is $0.344 \times 10^{-12}\ \text{mol}^{1-(a+b)}\,(\text{cm}^3)^{(a+b)}\,\text{s}^{-1}$ where $a = -0.9166$ and $b = 0.0530$. These calculations were described in Section 3.

This procedure requires a correct characterization of the mass transfer through the membrane contactor module, since the concentrations of each compound at the interfaces were estimated applying correlations of dimensionless number related to a particular geometry. The choice of an adequate correlation to describe hydrodynamic conditions at both sides of the membrane is the first requirement to obtain reliable results.

This method has been proposed in order to isolate the effect of the chelation at the interface obtaining the parameters of Eq. (4); the information concerning chemical aspects in this type of operations could be used with other hydrodynamic conditions in simulations without requirement of additional experimental runs.

6.2. Simulations of mass transfer: advantages and limitations of the described methodology

The mass transfer model developed in this work considers all steps applying a resistances-in-series approach to estimate the interfacial rate of the complex formation. This fact explains that the implementation of a simulation algorithm (described in Fig. 3) from those results to predict transmembrane flow of molybdenite gives a good agreement with experimental data. Fig. 4 shows predictions of transmembrane flow of molybdenite, which have been obtained by simulations and compared to the experimental ones reported by Valenzuela et al. [1].

The variability of experimental data used to correlate chemical kinetics and a correct choice of equations to estimate mass transfer coefficients in boundary layers can modify the predictive capacity of the mass transport model. However, under an adequate description of membrane contactor hydrodynamics, the model can extrapolate the transmembrane flow of the transferred compound and it can represent a rapid and accessible way to scale-up different membrane-based solvent extraction systems, especially when hollow fiber contactors are used. Nevertheless, the chemical mechanism for the complex formation at the interface cannot be identified with this methodology as it was explained in Section 6.1.

6.3. Real contribution of chemical kinetics on the overall mass transfer

The combined effect of the boundary layers and the complexation rate at the interface on the performance of extraction process

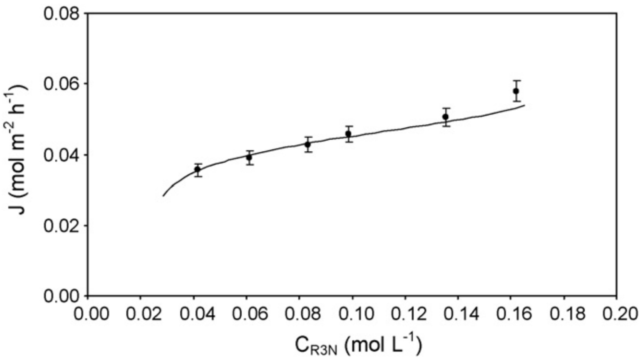

Fig. 4. Mean values of mass transfer flow of molybdenite (Mo(VI)) in function of the concentration (mol L^{-1}) of extractant (Alamine 336) obtained from experiments [1] and simulations using the algorithm described in Fig. 3 (this work). $T = 303$ K; $Q_{aq} = Q_{org} = 1.5 \times 10^{-2}$ mL s^{-1}.

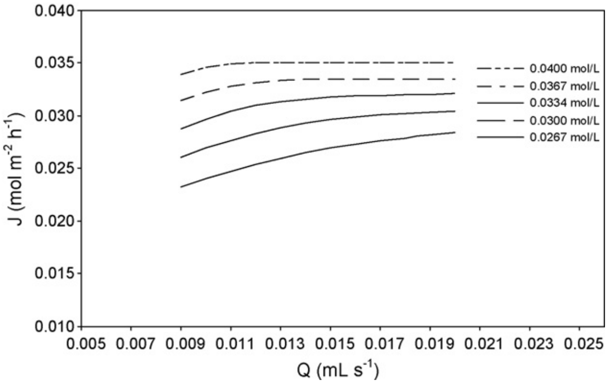

Fig. 5. Values of overall molybdenite (Mo(VI)) flow obtained from simulations in function of the circulation rates of both solutions. Concentration of molybdenite 1 g L^{-1}, T = 303 K. Concentration of Alamine 336 among 0.0267 and 0.040 mol L^{-1}.

may be observed in Fig. 5. This figure shows results obtained from simulations of mass transfer flow of Mo(VI) in function of the circulation rates of the aqueous and organic solution ($Q_{aq} = Q_{org}$, mL s^{-1}) for different values of concentration of extractant agent Alamine 336 in organic phase. The influence of the circulation rates on the mass transfer is observed when the concentration of Alamine 336 is lower 0.0334 mol L^{-1}. Over this value the transmembrane flow of Mo(VI) shows a plateau where the increase of the circulation rates of solutions does not involve an increase of transmembrane flow. This fact can be explained by the availability of Mo(VI) and extractant at the reaction interface. If the concentrations of the reactants at the interface become constants in function of the circulation rates, the mass transfer resistances represented by the boundary layers of the aqueous and organic solutions can be considered negligible compared to the resistance represented by the reaction rate. The maximum value of the mass transfer flow that can be obtained under specific conditions will be determined by the complexation rate and the diffusion conditions through the membrane pores.

The parametric study on influence of the process parameters based on the presented model has been done out of experimental interval of extractant concentrations, since under those experimental conditions the influence of the circulation rates of solution on the transmembrane flow was not significant.

6.4. Analysis of individual mass transfer resistances

The resistances-in-series model presented in this work allows the estimation of the concentrations for each species at the proximities of the fibers. In this way, it is possible to quantify the relative contribution of each individual mass transfer resistances as a function of the operation conditions as circulation rates of solutions or concentrations, and its influence on the transmembrane flow of Mo(VI).

Fig. 6 shows the calculated values of concentration of molybdenite at the interface on the aqueous solution side as a function of the circulation rate of the solutions for different values of concentration of extractant (Alamine 336) in the organic solution. When the circulation rate of the solutions and the concentration of extractant increase it is possible to observe a convergence of the curves on this figure. This convergence in the value of the concentration of molybdenite at the interface is explained by the condition of limiting reactant of this compound. The increase of the circulation rate minimizes the mass transfer resistance of the boundary layer of the aqueous solution, and then the concentration value of molybdenite at the interface is close to its bulk concentration.

On the other hand, the same increase of circulation rate was applied to the organic solution, minimizing the effect of the mass transfer resistance represented by its boundary layer in the proximities of the membrane. This effect was explained in Section 6.3. Nevertheless, Alamine 336 is not the limiting reactant in this system and its concentration at the aqueous–organic interface does not show convergence to a specific value when the circulation rate of solutions increases. This is shown in Fig. 7.

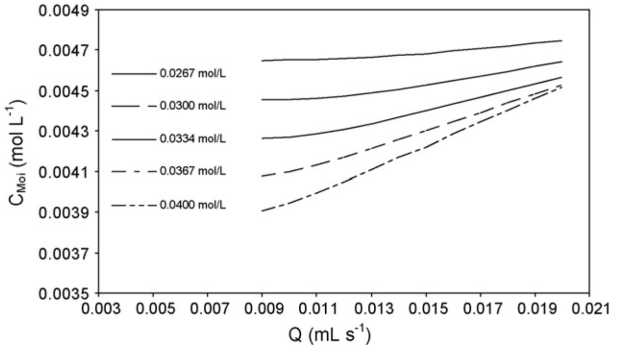

Fig. 6. Values of concentration of molybdenite (Mo(VI)) at the aqueous–organic interface obtained from simulations as a function of the circulation rates of both solutions for different values of concentrations of extractant agent (Alamine 336). Concentration of molybdenite 1.0 g L^{-1}, T = 303 K.

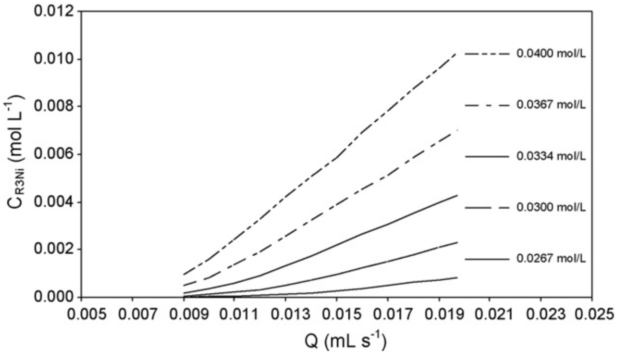

Fig. 7. Values of concentration of Alamine 336 at the aqueous–organic interface obtained from simulations as a function of the circulation rates of both solutions for different values of bulk concentrations of extractant agent (Alamine 336). Concentration of molybdenite 1.0 g L^{-1}, T = 303 K.

Under the operation conditions applied in this work, the relative contribution of the boundary layers to the overall mass transfer resistance decrease rapidly when the circulation rates are increased. High flows of solutions in this type of contactors generate a transmembrane flux controlled by the chemical kinetics and the diffusion through the membrane pores, but it is necessary to consider the stoichiometry, the rate, and the mechanisms of the reactions for specific applications.

Table 4 shows the values of fractional resistance of the respective step to the overall mass transport process obtained from Eqs. (14)–(17). These calculations were obtained under extreme condi-

Table 4
Mass transfer fractional resistances on a function of the circulation rates of the solutions and the concentration of Alamine 336. Fractional resistances for the aqueous boundary layer ($FR_{aqueous}$), the rate of the complex formation ($FR_{kinetic}$), the membrane pores ($FR_{membrane}$) and the organic boundary layer ($FR_{organic}$).

Variable concentration of extractant [R_3N] (mol L^{-1})	0.027	0.027	0.040	0.040
Volumetric rate, Q (mL s^{-1})	0.009	0.019	0.009	0.019
$FR_{aqueous}$ (%)	12.06	10.63	14.36	12.53
$FR_{kinetic}$ (%)	41.42	46.86	48.28	54.04
$FR_{membrane}$ (%)	24.55	28.07	19.73	22.07
$FR_{organic}$ (%)	21.97	14.44	17.63	11.36

tions, but the high value of fractional resistances of the chemical kinetics at the interface and the pores filled with organic phase can be verified, both individual resistances represent between 66 and 76% of the overall mass transfer resistance.

The improvement of the design of membrane contactor modules gives greater importance to the chemical kinetics aspects in the development of new membrane-based reactive extractions. The integration of transport phenomena, thermodynamics and chemical kinetics are necessary to describe these processes. The methodology described in this study is presented in order to simplify this analysis.

7. Conclusions

A study about the mass transfer of a membrane-based solvent extraction process to remove molybdenum(VI) from aqueous solutions was done in this work. The proposed approach considers a resistances-in-series model based on a group of mass transport equations, which has been applied to explain experimental data reported by Valenzuela et al. [1] extracting molybdenite from aqueous solutions with a solution of Alamine 336 in n-hexane as extraction phase using a hollow fiber contactor. An effective kinetics relationship was correlated in order to describe the rate of the complex formation at the aqueous–organic interface. This methodology allows obtaining a local quantification of the complex formation, which can be used to extrapolate or to scale-up this type of systems. Nevertheless, any mechanism cannot be directly inferred from these calculations.

The availability of the limiting reactant at the interface given by the hydrodynamic conditions in the membrane contactor and mass transfer in the membrane pores will establish the maximum transmembrane flux value. Under the operation conditions applied in this work, the mass transfer flow is controlled by the rate of the complex formation and the diffusion through the membrane pores.

The methodology described herein has been presented in order to simplify the analysis of the reactive extraction of Mo(VI). This approach could be applied to other membrane-based reactive extractions when its description needs the integration of phenomenological and kinetics aspects.

Acknowledgements

This work has been supported by the Project FONDECYT 1070062 (CONICYT Chile); the French-chilean collaboration program ECOS-Sud-CONICYT (Project C04 E06) and the University of Santiago de Chile. The financial support for the Ph.D. student Hugo Valdés is gratefully acknowledged.

References

[1] F. Valenzuela, H. Aravena, C. Basualto, J. Sapag, C. Tapia, Separation of Cu^{2+} and molybdenum(VI) from mine waters using two microporous extraction systems, Separation Science and Technology 35 (2000) 1409–1421.

[2] J.M. Mudre, J.J. Ney, Patterns of accumulation of heavy metals in the sediment of roadside streams, Journal Archives of Environmental Contamination and Toxicology 15 (1986) 489–493.

[3] K. Sreeram, R. Srinivasan, J. Devi, B. Nair, T. Ramasami, Cerium molybdenum oxides for environmentally benign pigments, Dyes and Pigments 75 (2007) 687–692.

[4] H. Al-Kandari, F. Al-Kharafi, A. Katrib, Catalytic activity-surface structure correlation of molybdenum-based catalysts, Journal of Molecular Catalysis A: Chemical 287 (2008) 128–134.

[5] P.C.H. Mitchell, The chemistry and uses of molybdenum: introductory lecture, Journal of the Less Common Metals 36 (1974) 3–11.

[6] K. Saberyan, M.G. Maragheh, P. Ashtari, S.K. Alamdari, Liquid–liquid extraction of molybdenum(VI) from acidic media with Cyanex-301, Minerals Engineering 16 (2003) 391–393.

[7] A.M. Sastre, F.J. Alguacil, Co-extraction and selective stripping of copper(II) and molybdenum(VI) using LIX 622, Chemical Engineering Journal 81 (2001) 109–112.

[8] A.A. Palant, N.A. Iatsenko, V.A. Petrova, Solvent extraction of molybdenum(VI) by diisododecylamine from sulphuric acid solution, Hydrometallurgy 48 (1998) 83–90.

[9] S.V. Vartak, V.M. Shinde, Separation studies of molybdenum(VI) and rhenium(VII) using TPPO as an extractant, Talanta 43 (1996) 1465–1470.

[10] J. Juneja, S. Singh, D. Bose, Investigations on the extraction of molybdenum and rhenium values from low grade molybdenite concentrate, Hydrometallurgy 41 (1996) 201–209.

[11] P. Zhang, K. Inoue, K. Yoshizuka, H. Tsuyama, Extraction and selective stripping of molybdenum(VI) and vanadium(IV) from sulfuric acid solution containing aluminum(III), cobalt(II), nickel(II) and iron(III) by LIX 63 in Exxsol D80, Hydrometallurgy 41 (1996) 45–53.

[12] J.J. Cruywagen, A.G. Draaijer, Solvent extraction investigation of molybdenum(VI) equilibria, Polyhedron 11 (1992) 141–146.

[13] T. Sato, H. Watanabe, H. Suzuki, Liquid–liquid extraction of molybdenum(VI) from aqueous acid solutions by TBP and TOPO, Hydrometallurgy 23 (1990) 297–308.

[14] J. Coca, F.V. Díez, M.A. Morís, Solvent extraction of molybdenum and tungsten by Alamine 336 and DEHPA, Hydrometallurgy 25 (1990) 125–135.

[15] K. Murata, S. Yamashita, E. Yamamoto, S. Ikeda, Extraction of molybdenum(VI) from aqueous solution by donor solvents, Polyhedron 9 (1990) 1717–1721.

[16] R. Basu, K.K. Sirkar, Non-dispersive membrane solvent back extraction of phenol, AIChE Journal 36 (1990) 450–460.

[17] R. Basu, K.K. Sirkar, Citric acid extraction with microporous hollow fibers, Solvent Extraction and Ion Exchange 10 (1992) 119–143.

[18] R. Basu, K.K. Sirkar, Pharmaceutical product recovery using a hollow fiber contained liquid membrane: a case study, Journal Membrane Science 75 (1992) 131–149.

[19] J.S. Gill, H. Singh, C.K. Gupta, Studies on supported liquid membrane for simultaneous separation of Fe(III), Cu^{2+} and Ni^{2+} from dilute feed, Hydrometallurgy 55 (2000) 113–116.

[20] Ch.E. Yang, L. Cussler, Reaction dependent extraction of copper and nickel using hollow fibers, Journal of Membrane Science 166 (2000) 229–238.

[21] R.-S. Juang, H.-L. Huang, Mechanistic analysis of solvent extraction of heavy metals in membrane contactors, Journal of Membrane Science 213 (2003) 125–135.

[22] J. Gyves, A.M. Hernández, E. Rodríguez, LIX®-loaded polymer inclusion membrane for $copper^{2+}$ transport. 2) Optimization of the efficiency factors (permeability, selectivity, and stability) for LIX® 84-I, Journal of Membrane Science 268 (2006) 142–149.

[23] Y. Wang, G. Luo, W. Cai, Y. Wang, Y. Dai, Membrane extraction for sulfanilic acid removal from wastewater, Separation Science and Technology 37 (2002) 1163–1177.

[24] L. Kubišová, E. Sabolová, Š. Schlosser, J. Marták, R. Kertész, Mass-transfer in membrane based solvent extraction and stripping of 5-methyl-2 pyrazinecarboxylic acid and co-transport of sulphuric acid in HF contactors, Desalination 163 (2004) 27–38.

[25] I. Souchon, V. Athès, F.-X. Pierre, M. Marin, Liquid–liquid extraction and air stripping in membrane contactor: application to aroma compounds recovery, Desalination 163 (2004) 39–46.

[26] M. Vajda, A. Kosuthova, S. Schlosser, Membrane-based solvent extraction and stripping of zinc in a hollow-fibre contactor operating in a circulating mode, Desalination 163 (2004) 19–25.

[27] S. Bocquet, F. Gascon, C. Muvdi, J. Sanchez, V. Athes, I. Souchon, Membrane-based solvent extraction of aroma compounds: choice of configuration of hollow fiber modules based on experiments and simulation, Journal of Membrane Science 281 (2006) 358–368.

[28] S. Kimura, S. Sourirajan, Mass transfer coefficients for use in reverse osmosis process design, National Research Council of Canada Ottawa (Ontario) Division of Applied Chemistry, 7 (October (4)), 1968.

[29] A. Urtiaga, M.J. Abellán, J.A. Irabien, I. Ortiz, Membrane contactors for the recovery of metallic compounds modelling of copper recovery from WPO processes, Journal of Membrane Science 257 (2005) 161–170.

[30] C.H. Yun, R. Prasad, A.K. Guha, K.K. Sirkar, Hollow fiber solvent extraction removal of toxic heavy metals from aqueous waste streams, Industrial and Engineering Chemistry 32 (1993) 1186–1195.

[31] Z.-F. Yang, A.K. Guha, K.K. Sirkar, Novel membrane-based synergistic metal extraction and recovery processes, Industrial and Engineering Chemistry 35 (1996) 1383–1394.

[32] F. Valenzuela, C. Fonseca, C. Basualto, O. Correa, C. Tapia, J. Sapag, Removal of copper ions from a waste mine water by a liquid emulsion membrane method, Minerals Engineering 18 (2005) 33–40.

[33] M.E. Campderrós, A. Acosta, J. Marchese, Selective separation of copper with LIX 864 in a hollow fiber module, Talanta 47 (1998) 19–24.

[34] R.S. Juang, L.J. Chen, Analysis of the transport rates of citric-acid through a supported liquid membrane containing tri-N-octylamine, Industrial & Engineering Chemistry Research 35 (1996) 1673.

[35] R.S. Juang, J.D. Jiang, Rate-controlling mechanism of cobalt transport through supported liquid membranes containing di(2-ethylhexyl)phosphoric acid, Separation Science and Technology 29 (1994) 223.

[36] R.S. Juang, I.P. Huang, Hollow-fiber membrane extraction of copper(II) from aqueous ethylenediaminetetraacetic acid-solutions with Aliquat-336, Industrial & Engineering Chemistry Research 39 (2000) 1409.

[37] R.S. Juang, I.P. Huang, Liquid–liquid extraction of copper(II)-EDTA chelated anions with microporous hollow fibers, Journal of Chemical Technology and Biotechnology 75 (2000) 610.

[38] S. Schlosser, R. Kertesz, J. Martak, Recovery and separation of organic acids by membrane-based solvent extraction and pertraction—an overview with a case study on recovery of MPCA, Separation and Purification Technology 41 (2005) 237.

[39] S. Schlosser, E. Sabolova, R. Kertesz, L. Kubisova, Factors influencing transport through liquid membranes and membrane based solvent extraction, Journal of Separation Science 24 (2001) 509.

[40] P.S. Kulkarni, V.V. Mahajani, Application of liquid emulsion membrane (LEM) process for enrichment of molybdenum from aqueous solutions, Journal of Membrane Science 201 (2002) 123–135.

[41] J. Marchese, F. Valenzuela, C. Basualto, A. Acosta, Transport of molybdenum with Alamine 336 using supported liquid membrane, Hydrometallurgy 72 (2004) 309–317.

[42] C. Basualto, J. Marchese, F. Valenzuela, A. Acosta, Extraction of molybdenum by a supported liquid membrane method, Talanta 59 (2003) 999–1007.

[43] F. Valenzuela, F. Pizarro, C. Basualto, J. Sapag, C. Tapia, Extracción de molybdenum(VI) con aminas terciarias en un reactor de membranes liquidas de soporte sólido, Boletín de la Sociedad Chilena de Química 46 (Junio (2)) (2001).

[44] F. Valenzuela, J. Andrade, J. Sapag, C. Tapia, C. Basualto, The solvent extraction separation of molybdenum and copper from acid leach residual solution of chilean molybdenite concentrate, Minerals Engineering 8 (1995) 893–904.

[45] A. Gabelman, S.-T. Hwang, Hollow fiber membrane contactors, Journal of Membrane Science 159 (1999) 61–106.

[46] D.J. Kathios, G.D. Jarvinen, S.L. Yarbro, B.F. Smith, A preliminary evaluation of microporous hollow fiber membrane modules for the liquid–liquid extraction of actinides, Journal of Membrane Science 97 (1994) 251–261.

[47] M.-C. Yang, E.L. Cussler, Designing hollow-fiber contactor, AIChE Journal 32 (1986) 1910–1916.

[48] R. Prasad, S. Khare, A. Sengupta, K.K. Sirkar, Novel liquid in-pore configurations in membrane solvent extraction, AIChE Journal 36 (1990) 1592–1596.

[49] H.Y. Lee, S.G. Kim, J.K. Oh, Development of kineticsequations for the extraction of copper by LIX65N based on interfacial reaction mechanism, Hydrometallurgy 34 (1994) 293–305.

[50] A. Irabien, I. Ortiz, E. Pérez, Kinetics of metal extraction: model discrimination and parameter estimation, Chemical Engineering and Processing 27 (1990) 13–18.

[51] E.N. Sieder, G.E. Tate, Heat transfer and pressure drop of liquids in tubes, Industrial and Engineering Chemistry 28 (1936) 1429.

[52] R. Bird, W. Stewart, E. Lightfoot, Transport Phenomena, 2nd edition, John Wiley & Sons Inc., USA, 2002.

[53] R. Viegas, M. Rodríguez, S. Luque, J. Alvarez, I. Coelhoso, J. Crespo, Mass transfer correlations in membrane extraction: analysis of Wilson-plot methodology, Journal of Membrane Science 145 (1998) 129–142.

[54] J. Kendall, K. Monroe, Journal of the American Chemical Society 39 (1917).